

Light anti-nuclei production in pp collisions at $\sqrt{s}=7$ and 14 TeV

Yu-Liang Yan¹, Gang Chen², Xiao-Mei Li¹, Dai-Mei Zhou³, Mei-Juan Wang², Shou-Yang Hu¹, Li Ye¹, Ben-Hao Sa^{1,3}

¹ *China Institute of Atomic Energy, P.O. Box 275(18), Beijing 102413, China*

² *Physics Department, China University of Geoscience, Wuhan 430074, China*

³ *Institute of Particle Physics, Huazhong Normal University, Wuhan 430082, China*

A dynamically constrained coalescence model based on the phase space quantization and classical limit method was proposed to investigate the production of light nuclei (anti-nuclei) in non-single diffractive (NSD) pp collisions at $\sqrt{s}=7$ and 14 TeV. This calculation was based on the final hadronic state in the PYTHIA and PACIAE model simulations, the event sample consisted of 1.2×10^8 events in both simulations. The PACIAE model calculated \overline{D} yield of 6.247×10^{-5} in NSD pp collisions at $\sqrt{s}=7$ TeV is well comparing with the ALICE rough datum of 5.456×10^{-5} . It indicated the reliability of proposed method in some extent. The yield, transverse momentum distribution, and rapidity distribution of the \overline{D} , ${}^3\overline{He}$, and ${}^3_{\Lambda}\overline{H}$ in NSD pp collisions at $\sqrt{s}=7$ and 14 TeV were predicted by PACIAE and PYTHIA model simulations. The yield resulted from PACIAE model simulations is larger than the one from PYTHIA model. This might reflect the role played by the parton and hadron rescatterings.

PACS numbers: 25.75.-q, 24.85.+p, 24.10.Lx

I. INTRODUCTION

The nucleus-nucleus collisions at top RHIC energy produced an initial hot and dense matter (quark-gluon matter, QGM) and has been interpreted as a strongly coupled quark-gluon plasma (sQGP) [1–4]. This is nearly a perfect liquid composed of quarks, antiquarks, and gluons but is not a free gas-like quark-gluon plasma (fQGP) expected by theorists and experimentalists long time ago.

We have proposed physical conjectures to theoretically explore the property differences among the QGM formed in pp and/or nucleus-nucleus collisions at ultra-relativistic energies [5]. These conjectures are: (1) The fraction of gluon in yield and momentum increases with increasing reaction energy. (2) The quark flavors (u, d, s, \dots) approach equilibrium with increasing reaction energy. (3) The antiparton to parton (u, d, s, \dots quarks) ratio increases with increasing reaction energy. In short, the population of u, d, s, c, \dots quarks and the antiquark to quark ratio approach equilibrium (balance) and unity with increasing reaction energy, respectively.

Recently STAR reported the observation of “an equilibrium in coordinate and momentum space populations of up, down, and strange quarks and antiquarks” by “The measured yields of ${}^3_{\Lambda}H$ (${}^3_{\Lambda}\overline{H}$) and 3He (${}^3\overline{He}$) are similar” or by the observation of ${}^3_{\Lambda}\overline{H}/{}^3_{\Lambda}H$ is close to ${}^3\overline{He}/{}^3He$ in Au+Au collisions at top RHIC energy [6]. Whether this STAR observation means the initial fireball created in this collision is really a fQGP may be debated.

The investigation of anti-nuclei has great meaning in the nuclear and particle physics, the astrophysics, and even in the cosmology. Recently ALICE published their preliminary results of \overline{D} production in pp collisions at $\sqrt{s}=7$ TeV [7] at nearly ten months later than STAR publishing their measurements for ${}^3_{\Lambda}\overline{H}$ production in

Au+Au collisions at $\sqrt{s_{NN}}=200$ GeV [6]. However, because of quite low multiplicity, the study of anti-nuclei production is very hard both in experiment and theory.

So far the report about the formation of QGM in early stage of pp collisions at RHIC energy is still absent in our knowledge. However, there were studies about the measurable of flow parameters and the elliptic flow signature of the QGP phase transition in high multiplicity (energy) pp collisions [8–13]. So one could not rule out the QGM formation possibility in pp collisions at LHC or higher energies [14].

In this paper the PYTHIA model [15] and PACIAE model [16] were used to calculate the final hadronic state in non-single diffractive (NSD) pp collisions at $\sqrt{s}=7$ and 14 TeV. That was followed by the calculations for the production of light anti-nuclei in the dynamically constrained coalescence model based on the phase space quantization and classical limit method. The PACIAE model calculated \overline{D} yield of 6.247×10^{-5} in NSD pp collisions at $\sqrt{s}=7$ TeV is well comparing with the ALICE rough datum of 5.456×10^{-5} . This may indicate the reliability of the proposed method in some extent. The parton and hadron rescattering effects were analyzed by comparing the PACIAE results with the PYTHIA one. It turned out that their role is un-negligible.

II. MODELS

PYTHIA is a model for high energy hadron-hadron (hh) collisions [15]. The parton and hadron cascade model, PACIAE [16], is based on PYTHIA. In the PYTHIA model a hh collision is decomposed into parton-parton collisions. The hard parton-parton collision is described by lowest leading order perturbative QCD (LO-pQCD) parton-parton interactions with the modification of parton distribution function in a hadron. The soft parton-parton collision, non-perturbative phenomenon,

is considered empirically. The initial- and final-state QCD radiations and multiparton interactions are considered. So the consequence of a hh collision is a partonic multijet state composed of di-quarks (anti-diquarks), quarks (antiquarks), and gluons, besides a few hadronic remnants. It is then followed by the string construction and fragmentation, one obtains a hadronic final state for a hh (pp) collision eventually.

For the pp collisions the PACIAE model is different from the PYTHIA in follows:

1. The string fragmentation is switched-off and the di-quarks (anti-diquarks) are broken randomly into quarks (antiquarks). So the consequence of a pp collision is a initial state of quarks, antiquarks, and gluons, besides a few hadronic remnants. This partonic initial state is regarded as the hot QCD matter (QGM) formed in the relativistic pp collisions.
2. The parton rescattering is introduced. In this stage the rescattering among partons in QGM is considered by the $2 \rightarrow 2$ LO-pQCD parton-parton interaction cross sections [17]. However, a K factor is introduced to consider the higher order and non-perturbative corrections. The effective strong coupling constant is assumed to be $\alpha_s=0.47$. A parton colour screen mass $\mu=0.63$ GeV is introduced to avoid the divergence. Integrate the differential cross sections above, the total cross section of the parton collision is obtained. Then the parton rescattering is simulated by the Monte Carlo method.
3. The hadronization is proceeded after parton rescattering. The partonic matter can be hadronized by the Lund string fragmentation regime [15] and/or phenomenological coalescence model [16].
4. At last the hadron rescattering is added. In this stage the hadronic matter after hadronization suffers rescattering. It is dealt with by the usual two-body collision method [18], until the hadronic freeze-out (the hh collision pair is exhausted).

In short, the PACIAE model consists of the parton initialization, parton evolution (rescattering), hadronization, and hadron evolution (rescattering) four stages.

STAR [6] has found in Au+Au collisions at top RHIC energy that “The measured $\frac{3}{\Lambda}\overline{H}/\frac{3}{\Lambda}H$ and $\frac{3}{\Lambda}\overline{He}/\frac{3}{\Lambda}He$ ratios are consistent with the interpretation that the $\frac{3}{\Lambda}\overline{H}$ and $\frac{3}{\Lambda}H$ are formed by coalescence of $(\overline{\Lambda} + \overline{p} + \overline{n})$ and $(\Lambda + p + n)$, respectively.” Obviously, this simplest coalescence assumption is utilized only for ratio and not for yield.

In the theoretical studies, the yield of light nuclei (anti-nuclei) was always calculated in two steps: In the first step the nucleons and hyperons were calculated by transport model. Then the light nuclei (anti-nuclei) were calculated by the analytical coalescence model [19–21] and/or the statistical model [22]. This meant the

formation of nuclei (hypernuclei) was not dynamically treated continuously but as a final state interaction separately. The above analytical coalescence model relies upon the Wigner function [23] constructed according to the assumed wave function of light nuclei (anti-nuclei) [21]. The statistical model relies upon the equilibrium and temperature assumptions as well as the restriction on projectile-like fragment in the intermediate energy heavy ion collisions. In this paper we proposed a dynamically constrained coalescence model based on the phase space quantization and classical limit method to calculate the yield of light nuclei (anti-nuclei) after the transport model simulation directly.

One knew in statistical mechanics [24] that, for a system with three dimensions in the state definition the set of microscopic states held in a volume element $\Delta\Gamma$ corresponds, in the limit of $h \rightarrow 0$, to a set of

$$\frac{\Delta\Gamma}{h^3} \quad (1)$$

quantum states. Of course, this correspondence is an approximation as long as h remains finite. In the Eq. 1 $\Delta\Gamma$ reads

$$\Delta\Gamma \equiv \Delta\vec{q}\Delta\vec{p} \quad (2)$$

where \vec{q} and \vec{p} stand for the three position and three momentum, respectively. In other word, a h^3 volume element in the three dimensions phase space corresponds to a state of the system.

III. CALCULATIONS AND RESULTS

Taking the system of $\frac{3}{\Lambda}\overline{H}$ as an example, a configuration consists of \overline{p} , \overline{n} , and $\overline{\Lambda}$ in a single event of the final hadronic state from transport model simulation could be expressed as

$$C_{\overline{p}\overline{n}\overline{\Lambda}}(q_1, q_2, q_3; \vec{p}_1, \vec{p}_2, \vec{p}_3), \quad (3)$$

where subscripts 1, 2, and 3 were a shorthand for \overline{p} , \overline{n} , and $\overline{\Lambda}$, respectively and q_1 refers to the distance between \overline{p} and the center-of-mass of \overline{p} , \overline{n} , and $\overline{\Lambda}$, for instance. This configuration contributed an partial yield of

$$\delta_{123} = \begin{cases} 1 & \text{if } m_{inv} \leq m_0 \pm \Delta m, \quad q_1 \leq R_0, \\ & q_2 \leq R_0, \quad q_3 \leq R_0; \\ 0 & \text{otherwise;} \end{cases} \quad (4)$$

to the $\frac{3}{\Lambda}\overline{H}$. In the above equation

$$m_{inv} = [(E_1 + E_2 + E_3)^2 - (\vec{p}_1 + \vec{p}_2 + \vec{p}_3)^2]^{1/2} \quad (5)$$

is the invariant mass, m_0 and R_0 stand for the rest mass and radius of the $\frac{3}{\Lambda}\overline{H}$, Δm refers to the allowed mass uncertainty. The total yield of $\frac{3}{\Lambda}\overline{H}$ in a single event is the sum of above partial yield first over the Eq. 3 type

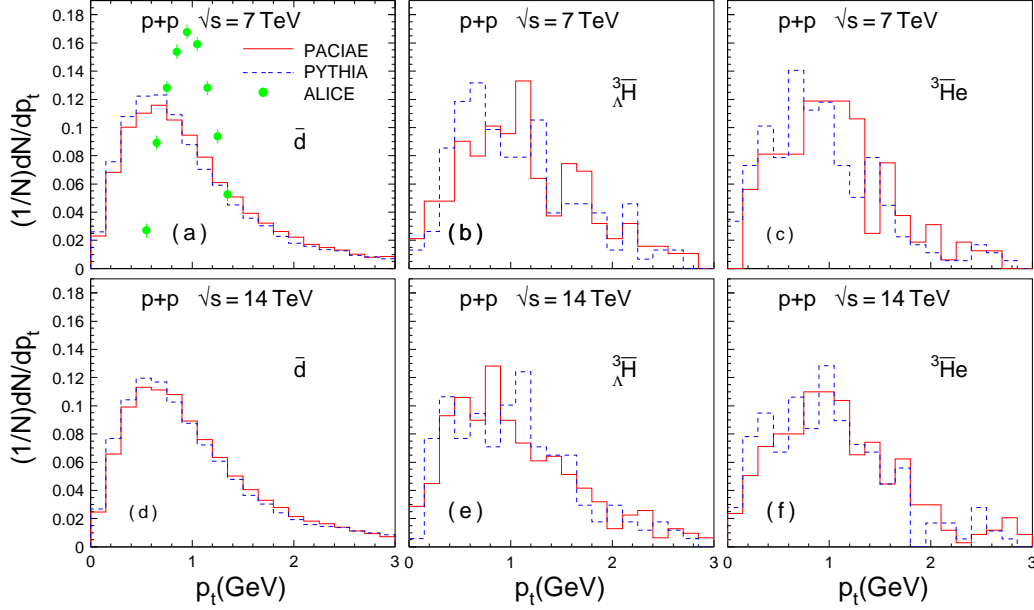


FIG. 1: (Color online) Light anti-nuclei transverse momentum distributions in the NSD pp collisions at $\sqrt{s}=7$ and 14 TeV. The panels (a), (b), and (c) were for \bar{D} ($\Delta m=0.0005$ GeV), $\bar{\Lambda}^3$ ($\Delta m=0.005$ GeV), and \bar{He}^3 ($\Delta m=0.005$ GeV), respectively, in the NSD pp collisions at $\sqrt{s}=7$ TeV, the panels (d), (e), and (f) at $\sqrt{s}=14$ TeV. The red solid and blue dashed histograms were calculated by final hadronic state in PACIAE and PYTHIA model simulations, respectively.

TABLE I: Particle yield in NSD pp collisions at $\sqrt{s}=0.2$ TeV.

	STAR ^a	PACIAE	PYTHIA
k^+	0.140 ± 0.010	0.137	0.125
k^-	0.137 ± 0.009	0.122	0.115
Λ	0.0385 ± 0.0036	0.0382	0.0309
$\bar{\Lambda}$	0.0351 ± 0.0033	0.0381	0.0312

^a The STAR data were taken from [26]

configurations and then over the configuration types obtained by the combination among subscripts 1, 2, and 3. An average over events is required at last.

The above summation was easily practised by following algorithm: One devised a three level loops (i , j , and k) over particle list in a single event of the final hadronic state from transport model simulation. If the particle code [25] (KF code in PYTHIA model [15]) sum of the three particles (i , j , and k) was equal to -7446 (= -2212-2112-3122) and the condition of Eq. 4 was satisfied then the $\bar{\Lambda}^3$ yield increased by one unit. The loops was then proceeded by jumping to i loop, the regular loop proceeding otherwise.

In the PYTHIA and PACIAE simulations we assumed that the hyperons heavier than Λ will decay. The model

parameters were fixed on the default values given in PYTHIA model, except the K factor and the parameters of $\text{parj}(1)$, $\text{parj}(2)$, and $\text{parj}(3)$ (the later three were concerning in hyperon production [15]) were roughly fitted to the STAR data of k^+ , k^- , Λ , and $\bar{\Lambda}$ in NSD pp collisions at $\sqrt{s}=0.2$ TeV [26] as shown in Tab. I. The fitted parameter values of 3 (default value is 1 or 1.5), 0.15 (0.1), 0.38 (0.3), and 0.45 (0.4) were used to calculate the yield of \bar{D} , \bar{He}^3 , and $\bar{\Lambda}^3$ in NSD pp collisions at $\sqrt{s}=7$ and 14 TeV by the final hadronic state in PACIAE and PYTHIA model simulations as shown in Tab. II.

One sees in the Tab. II that:

- The \bar{D} yield of 6.247×10^{-5} in NSD pp collisions at $\sqrt{s}=7$ TeV in the PACIAE simulations seems reasonable comparing with the ALICE rough datum of $\sim 5.456 \times 10^{-5}$ (roughly estimated from Fig. 4 in [7] where integrating over p_t and dividing by 350 M triggered events measured). The value in the PACIAE model larger than ALICE datum may attribute to the full rapidity phase space in the former (the same in all calculations in both PACIAE and PYTHIA models) but $|\eta| < 0.9$ in the later.
- The PACIAE yield of anti-hadron increases with increasing reaction energy from 7 TeV to 14 TeV in a percentage of $\sim 20\%$. It is less than the light anti-nuclei ($\sim 37\%$ for \bar{D} , $\sim 50\%$ for $\bar{\Lambda}^3$, and $\sim 70\%$ for \bar{He}^3). This might attribute to the available phase space increases with increasing reaction energy is

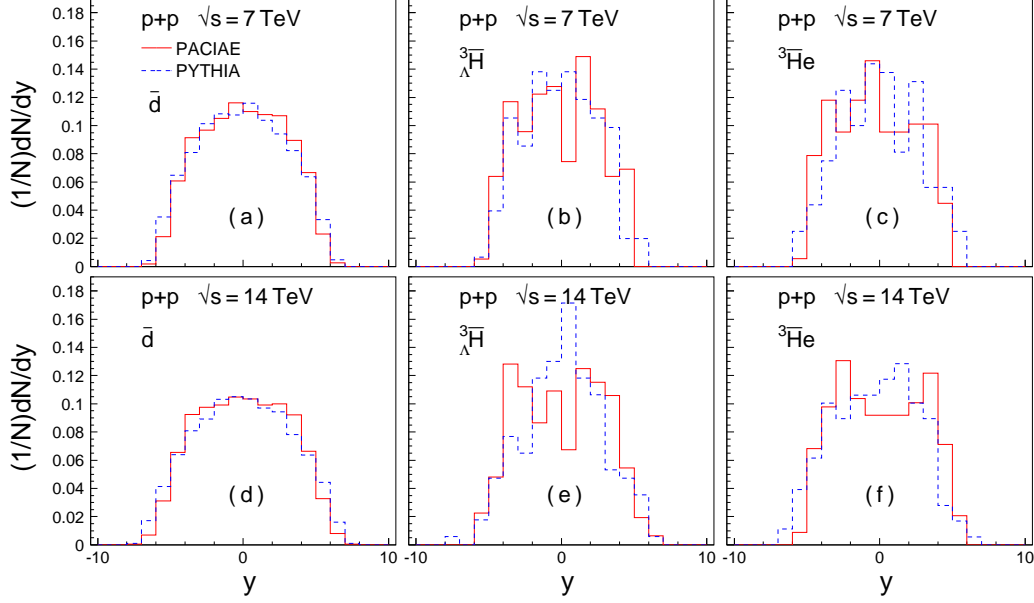


FIG. 2: (Color online) The same as Fig. 1 but for rapidity.

TABLE II: Hadron and light nuclei (anti-nuclei) yields in NSD pp collisions at $\sqrt{s}=7$ and 14 TeV calculated by final hadronic state in the PACIAE and PYTHIA model simulations.

	PACIAE		PYTHIA	
	7 TeV	14 TeV	7 TeV	14 TeV
k^+	4.563	5.576	3.802	4.946
k^-	4.416	5.331	3.689	4.778
p	4.152	4.678	3.491	4.074
\bar{p}	3.040	3.588	2.472	3.078
n	4.094	4.677	3.397	4.107
\bar{n}	3.336	3.938	2.565	3.335
Λ	1.648	1.940	1.285	1.608
$\bar{\Lambda}$	1.518	1.769	1.136	1.386
D^a	6.906E-05	9.111E-05	5.586E-05	6.724E-05
\bar{D}^a	6.247E-05	8.553E-05	4.852E-05	6.048E-05
	5.456E-05 ^b			
${}^3_\Lambda H^c$	2.547E-07	3.814E-07	1.833E-07	9.677E-08
${}^3_{\bar{\Lambda}} \bar{H}^c$	2.453E-07	3.305E-07	1.000E-07	1.048E-07
${}^3He^c$	2.453E-07	3.898E-07	1.500E-07	1.774E-07
${}^3\bar{H}^c$	2.642E-07	4.407E-07	1.417E-07	2.419E-07

^a Calculated with $\Delta m=0.0005$ GeV.

^b Estimated from Fig. 4 in [7].

^c Calculated with $\Delta m=0.005$ GeV.

stronger in the light anti-nuclei production rather than in the anti-hadron production.

- The yield resulted from PACIAE model simulation is larger than the one from PYTHIA model simula-

tion at the same reaction energy. This reflects the role played by the parton and hadron rescatterings.

Table III showed the feature of average transverse momentum of the produced light nuclei (anti-nuclei) is not sensitive to the special piece of nuclei (anti-nuclei) and the reaction energy, like the case of hadron production. However, the $\langle p_t \rangle$ seems to be ~ 1 GeV/c in light nuclei (anti-nuclei) production instead of ~ 0.5 GeV/c in hadron production. This might mean the light nuclei (anti-nuclei) are generated more isotropically in the momentum phase space.

Figure 1 gave the predicted \bar{D} ($\Delta m=0.0005$ GeV), ${}^3_{\bar{\Lambda}} \bar{H}$ ($\Delta m=0.005$ GeV), and ${}^3\bar{H}e$ ($\Delta m=0.005$ GeV) transverse momentum distributions in NSD pp collisions at $\sqrt{s}=7$ and 14 TeV. The panel (a) was for \bar{D} where the ALICE data [7] were also given by the green circles. One sees in this panel that the dN/dp_t shape in PACIAE and/or PYTHIA model simulations is similar to the one in general hadron production. The experimental Gaussian-like dN/dp_t may be modified after “efficiency and annihilation corrections” [7]. The Fig. 1 show that the 1.2×10^8 events are enough for dN/dp_t distribution of \bar{D} but not enough for ${}^3_{\bar{\Lambda}} \bar{H}$ and ${}^3\bar{H}e$. This was also the reason using different Δm value in the calculations for \bar{D} and for ${}^3_{\bar{\Lambda}} \bar{H}$ and ${}^3\bar{H}e$. The larger fluctuation are shown in panels (b), (c), (e), and (f). Globally speaking, the PACIAE dN/dp_t distribution is not so much different from the PYTHIA one.

We also predicted the rapidity distribution for the \bar{D} , ${}^3_{\bar{\Lambda}} \bar{H}$, and ${}^3\bar{H}e$ in NSD pp collisions at $\sqrt{s}=7$ and 14 TeV in Fig. 2. In this figure one sees that the global features shown in dN/dy distribution are quite similar to

the dN/dp_t distribution in Fig. 1 so need not to repeat.

TABLE III: Light nuclei (anti-nuclei) average transverse momentum in NSD pp collisions at $\sqrt{s}=7$ and 14 TeV calculated by final hadronic state in the PACIAE and PYTHIA model simulations.

	PACIAE		PYTHIA	
	7 TeV	14 TeV	7 TeV	14 TeV
D	0.988	0.993	0.941	0.952
\overline{D}	0.999	1.01	0.955	0.981
	0.962 ^a		0.955 ^a	
${}^3_{\Lambda}H$	1.07	1.05	0.909	1.01
${}^3_{\Lambda}\overline{H}$	1.14	1.05	1.09	1.00
3He	1.05	1.07	0.983	1.04
${}^3\overline{He}$	0.939	1.10	1.05	1.05

^a Estimated according to the Fig. 4 in [7].

IV. CONCLUSION

In summary, the PYTHIA model and the parton and hadron cascade model PACIAE based on PYTHIA

were employed to investigate the production of light nuclei (anti-nuclei) in NSD pp collisions at $\sqrt{s}=7$ and 14 TeV. We proposed a dynamically constrained coalescence model based on the phase space quantization and classical limit method to calculate the light nuclei (anti-nuclei) by the final hadronic state in PACIAE (PYTHIA) model simulations. The calculated \overline{D} yield of 6.247×10^{-5} in NSD pp collisions at $\sqrt{s}=7$ TeV by PACIAE model final hadronic state is quite close to the ALICE rough datum of 5.456×10^{-5} [7]. It turned out the reliability of proposed method in some extent. The light nuclei (anti-nuclei) yield, rapidity distribution, and transverse momentum distribution in NSD pp collisions at $\sqrt{s}=7$ and 14 TeV were also predicted by PACIAE and PYTHIA model simulations. The yield resulted from the PACIAE model simulations is larger than the one from PYTHIA model which might reflect the role played by the parton and hadron rescatterings.

ACKNOWLEDGMENT

Finally, we acknowledge the financial support from NSFC (11075217, 11047142, and 10975062) in China.

-
- [1] I. Arsene, et al., BRAHMS Collaboration, Nucl. Phys. A **757**, 1 (2005).
 - [2] B. B. Back, et al., PHOBOS Collaboration, Nucl. Phys. A **757**, 28 (2005).
 - [3] J. Admas, et al., STAR Collaboration, Nucl. Phys. A **757**, 102 (2005).
 - [4] K. Adcox, et al., PHENIX Collaboration, Nucl. Phys. A **757**, 184 (2005).
 - [5] Ben-Hao Sa, Dai-Mei Zhou, Yu-Liang Yan, Bao-Guo Dong, Hai-Liang Ma, and Xiao-Mei Li, Nucl. Phys. A **834**, 309c (2010).
 - [6] The STAR Collaboration, Science **328**, 58 (2010); arXiv:1003.2030v1.
 - [7] N. Sharma, ALICE Collaboration, arXiv:1104.3311v1.
 - [8] J. Casalderrey-Solana and U. A. Wiedemann, Phys. Rev. Lett. **104**, 102301 (2010).
 - [9] T. J. Humanic, arXiv:0902.0932v1.
 - [10] P. Bozek, arXiv:0911.2392v1.
 - [11] G. Ortona, G. S. Denicol, Ph. Mota, and T. Kodama, arXiv:0911.5158v1.
 - [12] A. K. Chaudhuri, arXiv:0912.2578v2.
 - [13] Dai-Mei Zhou, Yu-Liang Yan, Bao-Guo Dong, Xiao-Mei Li, Du-Juan Wang, Xu Cai, and Ben-Hao Sa, Nucl. Phys. A **860** 61 (2011).
 - [14] N. Armesto, M. A. Braun, and C. Pajares, Phys. Rev. C **75**, 054902 (2007).
 - [15] T. Sjöstrand, S. Mrenna, and P. Skands, J. High Energy Phys. **JHEP05**, 026 (2006).
 - [16] Yu-Liang Yan, Dai-Mei Zhou, Bao-Guo Dong, Xiao-Mei Li, Hai-Liang Ma, and Ben-Hao Sa, Phys. Rev. C **81** 044914 (2010); Ben-Hao Sa, Dai-Mei Zhou, Yu-Liang Yan, Xiao-Mei Li, Sheng-Qin Feng, Bao-Guo Dong, and Xu Cai, arXiv:1104.1238v1.
 - [17] B. L. Combridge, J. Kripfgang, and J. Ranft, Phys. Lett. B **70**, 234 (1977).
 - [18] Ben-Hao Sa and Tai An, Comput. Phys. Commun. **90**, 121 (1995); Tai An and Ben-Hao Sa, Comput. Phys. Commun. **116**, 353 (1999).
 - [19] R. Mattiello, H. Sorge, H. Stöcker, and W. Greiner, Phys. Rev. C **55** 1443 (1997).
 - [20] Lie-Wen Chen and Che Ming Ko, Phys. Rev. C **73** 044903 (2006).
 - [21] S. Zhang, J. H. Chen, H. Crawford, D. Keane, Y. G. Ma, and Z. B. Xu, Phys. Lett. B **684**, 224 (2010), and references therein.
 - [22] V. Topor Pop and S. Das Gupta, Phys. Rev. C **81** 054911 (2010), and references therein.
 - [23] E. Wigner, Phys. Rev. **40**, 749 (1932).
 - [24] R. Kubo, Statistical Mechanics, North-Holland Publishing Company, Amsterdam, 1965.
 - [25] Particle Data Group, Review of Particle Physics, J. Phys. G: Nucl. and Part. Phys. **37** 075021 (2010).
 - [26] B. I. Abelev, et al., STAR Collaboration, Phys. Rev. C **75** 064901 (2007).